

Molecular Cell, Volume 52

Supplemental Information

A Bacterial Toxin Inhibits DNA Replication Elongation through a Direct Interaction with the β Sliding Clamp

Christopher D. Aakre, Tuyen N. Phung, David Huang, and Michael T. Laub

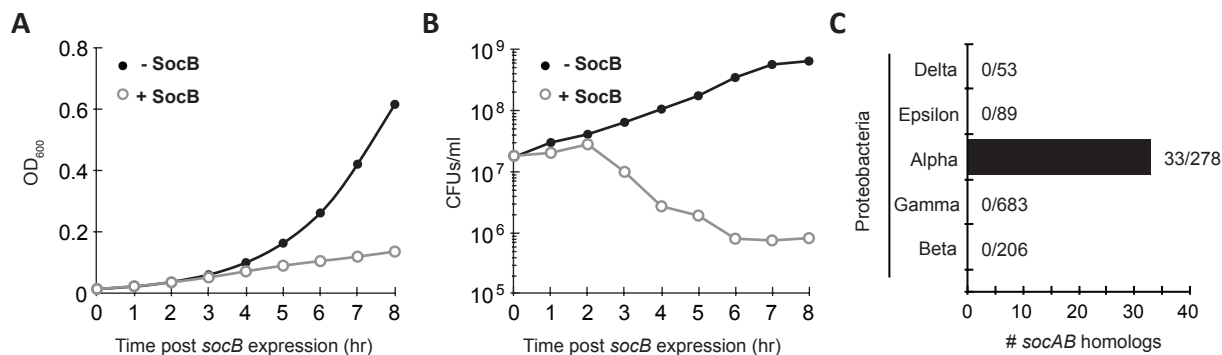


Figure S1. Effects of SocB Production on Viability; Evolutionary Conservation of *socAB*, Related to Figure 1

(A) Growth curve of $\Delta socAB$ P_{xyI} - $socA$ P_{van} - $socB$ cells following induction of *socB* expression at time zero.

(B) Measurement of colony-forming units (CFUs) from growth curve in (A). At each time point, cells were plated onto medium containing xylose to induce *socA* expression and neutralize any remaining SocB.

(C) Number of *socAB* homologs in each class of proteobacteria. Homologs were identified by a modified version of reciprocal best hit against fully sequence genomes in the IMG database (September 2012). *socA* and *socB* homologs were first identified independently by reciprocal best hit in each bacterial genome. Afterward, *socA* homologs that also had a *socB* homolog directly downstream were called as *socAB* homologs. Numbers next to each bar indicate number of homologs / number of total species searched.

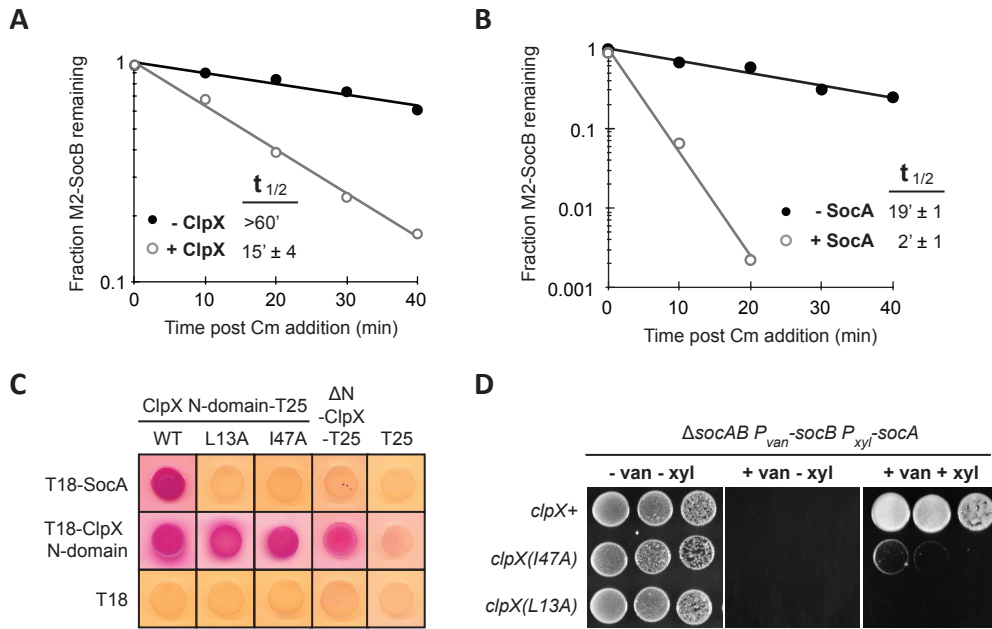


Figure S2. Quantification of M2-SocB Stability; Interaction of SocA with ClpX N-Domain Required for Antitoxin Activity, Related to Figure 2

(A-B) Quantification of (A) M2-SocB stability \pm ClpX (from Figure 2B) or (B) M2-SocB stability \pm SocA (from Figure 2D). The average M2-SocB band intensity from three biological replicates was measured and plotted to calculate protein half-life.

(C) SocA interacts with the ClpX N-domain, and mutations in the ClpX N-domain can abolish this interaction. Candidate residues in the ClpX N-domain were chosen based on the crystal structure of the *E. coli* ClpX N-domain in complex with the adaptor SspB (PDB ID: 2DS8) under the assumption that SocA and SspB may bind the ClpX N-domain in a similar fashion. We mutated a series of residues in the ClpX N-domain that directly contact SspB, and found that two mutations, L13A and I47A, were sufficient to abolish the ClpX N-domain-SocA interaction. Bacterial two-hybrid interaction is shown between the ClpX N-domain (residues 1-62), ClpX N-domain mutants, Δ N-ClpX (residues 63-420), and SocA. Dimerization between the ClpX N-domain is included as a control, to demonstrate that the L13A and I47A mutations specifically disrupted the SocA-N-domain interaction. Cells were grown for 2 days at 30°C.

(D) Interaction of SocA with ClpX N-domain is required for SocA to function as an antitoxin *in vivo*. We generated a chromosomal replacement of *clpX* with *clpX(L13A)* or *clpX(I47A)*, which are mutations that abolish the ability of ClpX to interact with SocA (Figure S2C). We then spotted the indicated strains on media that represses both *socA* and *socB* (-van -xyl), induces only *socB* (+van -xyl), or induces both *socA* and *socB* (+van +xyl). Five-fold serial dilutions are shown.

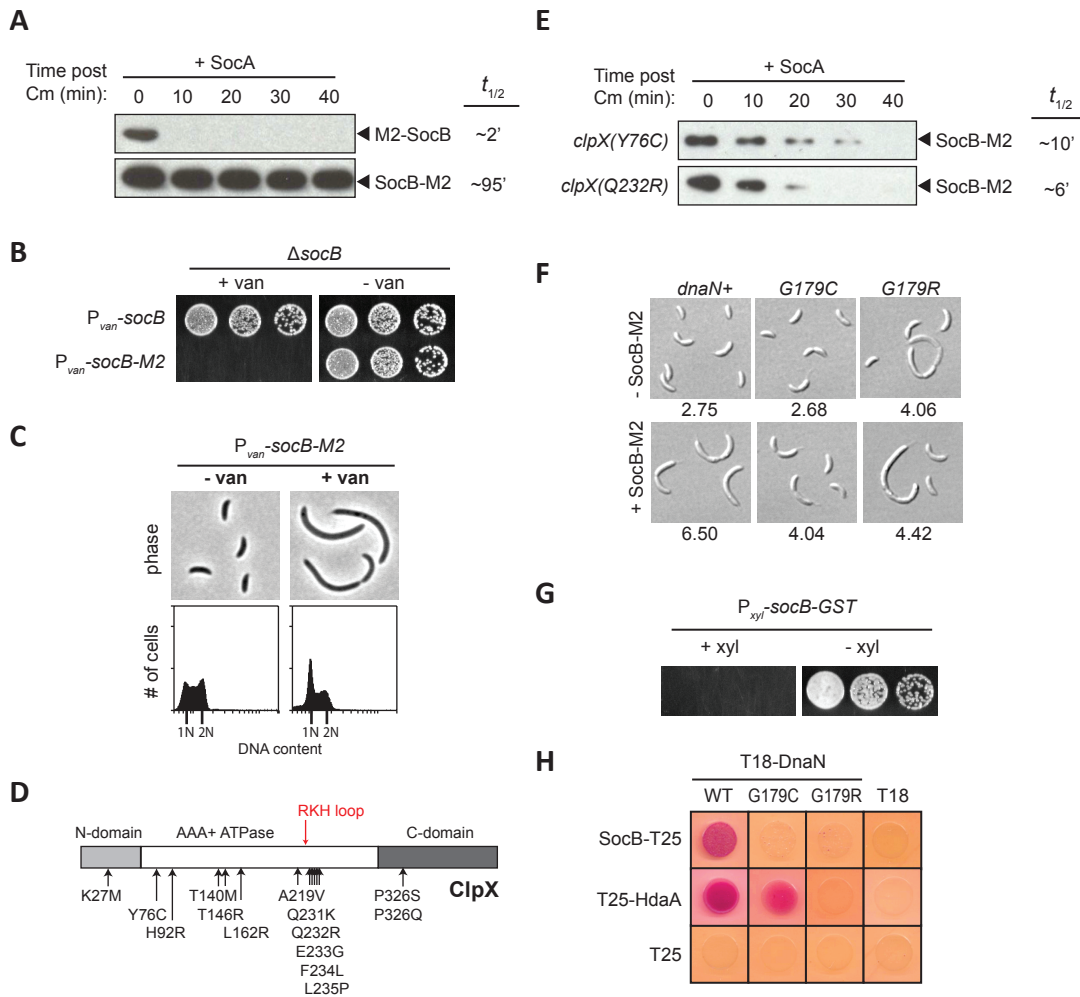


Figure S3. Suppressor Mutations in *clpX* That Destabilize SocB-M2; Phenotype of Suppressors in *dnaN*; Interaction Data Between SocB, DnaN, and HdaA, Related to Figure 3

(A) Stability of M2-SocB or SocB-M2 in the presence of SocA. *M2-socB* or *socB-M2* expression was induced for 2 hr, and then *socA* expression was induced for an additional 40 min prior to Cm addition at time zero to shut off protein synthesis. Half-life was quantified from two replicates.

(B) Growth of indicated strains on media that induces (+van) or represses (-van) expression of *socB* or *socB-M2*. Five-fold serial dilutions are shown.

(C) Phase microscopy and DNA content of the indicated strain in the absence or presence of *socB-M2* expression for 6 hr.

(D) Schematic of ClpX protein with mutations that bypass the toxicity of *socB-M2* expression indicated by arrows. Most mutations cluster near the RKH loop that is important for the recognition of *ssrA*-tagged substrates.

(E) Stability of SocB-M2 in the presence of SocA in the *clpX(Y76C)* and *clpX(Q232R)* backgrounds. Performed as in Fig. S3A.

(F) Morphology, assessed by DIC microscopy, of indicated strains after 4 hr of growth in medium that induces or represses *socB-M2* expression. Average cell length (μm) is shown below each panel ($n > 300$ cells).

(G) Growth of indicated strain on media that induces (+xyl) or represses (-xyl) expression of *socB-GST*. Five-fold serial dilutions are shown.

(H) Bacterial two-hybrid analysis of the interactions between DnaN, DnaN mutants, SocB, and HdaA. Cells were grown for 2 days at 30°C.

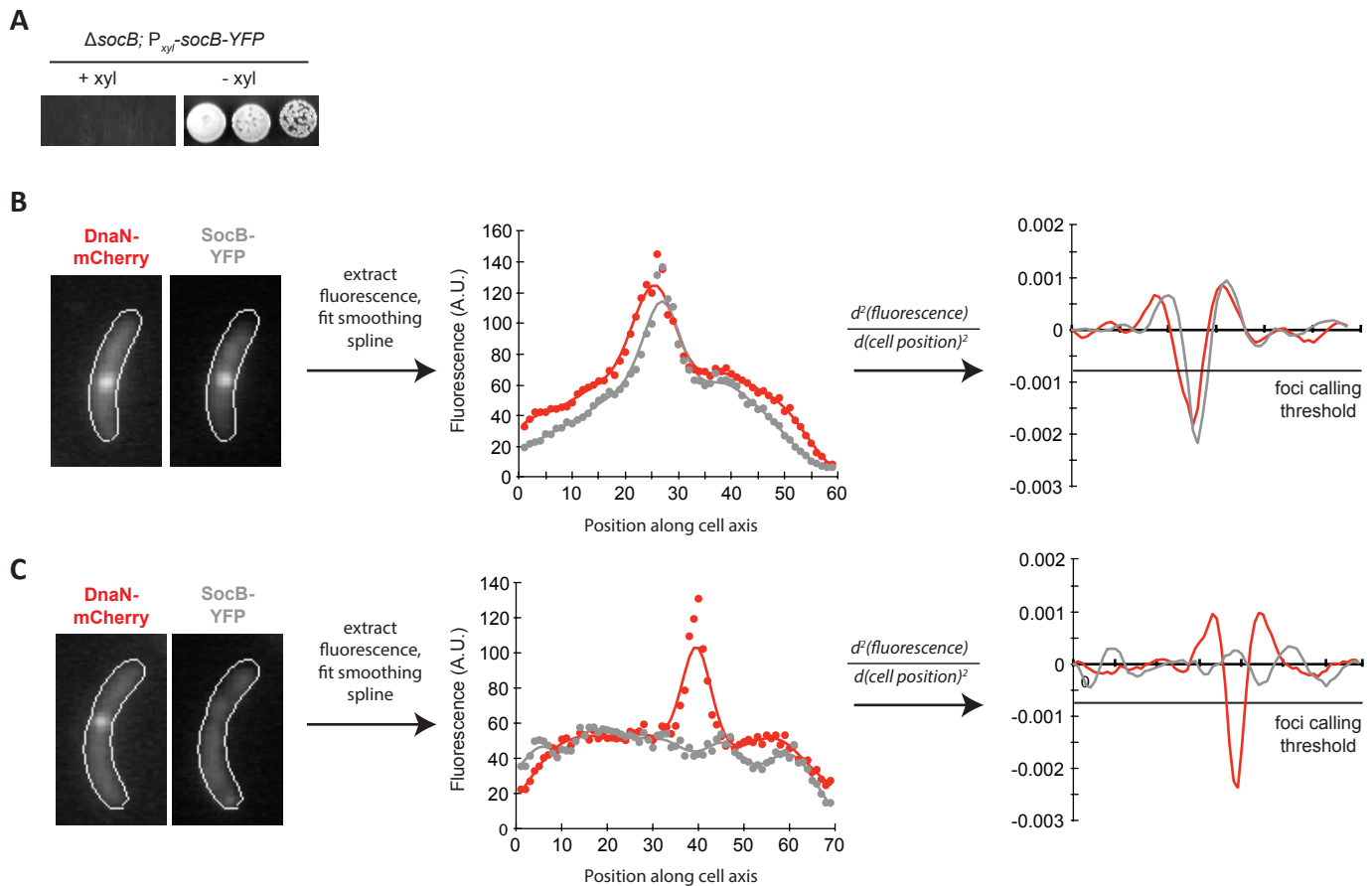


Figure S4. Toxicity of *socB*-YFP Expression; Workflow for Automated Co-Localization Calling, Related to Figure 5

(A) Growth of indicated strain on media that induces (+xyl) or represses (-xyl) *socB*-YFP expression. Five-fold serial dilutions are shown.

(B) Example cell exhibiting co-localization. Cells are first segmented and fluorescence signal extracted along the main cell axis. A smoothing spline is fit to the fluorescence signal and the second derivative of the fit is plotted. Local minima in the second derivative indicate “peaks” in the fluorescence signal; thus, the depth of the local minimum is a measure of the sharpness of the peak. Local minima that cross below a pre-determined threshold are called as foci, and cells are marked as co-localization positive if (1) the cell has foci for both DnaN-mCherry and SocB-YFP, and (2) the local minima in the second derivative for DnaN-mCherry and SocB-YFP overlap.

(C) Example cell not exhibiting co-localization; methodology is the same as in (A). This cell is co-localization negative because no significant minima are detected in the second derivative of the SocB-YFP signal.

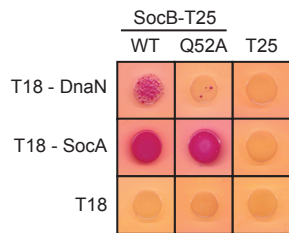


Figure S5. Interaction Between SocB, SocB(Q52A), and SocA, Related to Figure 6

Bacterial two-hybrid analysis of the interaction between SocB, SocB(Q52A), DnaN, and SocA. Cells were grown for 2 days at 30°C.

Supplemental Table 1 - Strains

Strain #	Genotype	Source
UJ199	$\Delta clpP$; $P_{xyl-clpP}::tet^R$ (<i>xyl</i> locus)	(Jenal and Fuchs, 1998)
ML2029	$\Delta clpP$; pMR20: $P_{lacI-lacI-P_{lac-clpP}}::tet^R$	This study
ML2030	$\Delta clpX$; pMR20: $P_{lacI-lacI-P_{lac-clpX}}::tet^R$	This study
ML2031	$\Delta clpP$; $\Delta socB$; pMR20: $P_{lacI-lacI-P_{lac-clpP}}::tet^R$	This study
ML2032	$\Delta clpX$; $\Delta socB$; pMR20: $P_{lacI-lacI-P_{lac-clpX}}::tet^R$	This study
ML2033	$\Delta socB$; $P_{van-socB}::kan^R$	This study
ML2034	$\Delta socAB$; $P_{van-socB}::kan^R$	This study
ML2035	$\Delta socAB$; $P_{van-socB}::kan^R$; pMR20: $P_{xyl-socA}::tet^R$	This study
ML2036	$\Delta clpX$; $\Delta socB$; pMR20: $P_{lacI-lacI-P_{lac-clpX}}::tet^R$; $P_{van-M2-socB}::kan^R$	This study
ML2037	$\Delta clpX$; $\Delta socB$; pMR20: $P_{lacI-lacI-P_{lac-clpX}}::tet^R$; pJS14: $P_{xyl-M2-socB}::chlor^R$	This study
ML2038	$\Delta socB$; pMR20: $P_{xyl-M2-socB}::tet^R$	This study
ML2039	$\Delta socAB$; pMR20: $P_{xyl-M2-socB}::tet^R$	This study
ML2040	$\Delta socAB$; $P_{van-M2-socB}::kan^R$; pMR20: $P_{xyl-socA}::tet^R$	This study
ML2041	$clpX(I47A)$; $\Delta socAB$; $P_{van-socB}::kan^R$; pMR20: $P_{xyl-socA}::tet^R$	This study
ML2042	$clpX(L13A)$; $\Delta socAB$; $P_{van-socB}::kan^R$; pMR20: $P_{xyl-socA}::tet^R$	This study
ML2044	$\Delta socB$; pMR20: $P_{xyl-socB-M2}::tet^R$	This study
ML2045	$\Delta socB$; $P_{van-socB-M2}::kan^R$	This study
ML2046	$dnaN(G179C)$; $\Delta socB$; $P_{van-socB-M2}::kan^R$	This study
ML2047	$dnaN(G179R)$; $\Delta socB$; $P_{van-socB-M2}::kan^R$	This study
ML2048	$\Delta socB$; $P_{xyl-socB-M2}::gent^R$; pRVYFPC-5: $P_{van-dnaN-YFP}::tet^R$	This study
ML2049	$dnaN(G179C)$; $\Delta socB$; $P_{xyl-socB-M2}::gent^R$; pRVYFPC-5: $P_{van-dnaN(G179C)-YFP}::tet^R$	This study
ML2050	$\Delta socB$; $P_{xyl-socB-YFP}::kan^R$ (<i>xyl</i> locus)	This study
ML2051	$dnaN(G179C)$; $\Delta socB$; $P_{xyl-socB-YFP}::kan^R$ (<i>xyl</i> locus)	This study
ML2052	$dnaN(G179R)$; $\Delta socB$; $P_{xyl-socB-YFP}::kan^R$ (<i>xyl</i> locus)	This study
ML2053	$P_{lacI-lacI}$ (<i>hfaA</i> locus); $P_{lac-dnaA}$ (<i>dnaA</i> locus); $P_{xyl-socB-YFP}::kan^R$ (<i>xyl</i> locus)	This study
ML2054	$\Delta socB$; $P_{xyl-socB-YFP}::kan^R$ (<i>xyl</i> locus); $dnaN-mCherry::gent^R$ (native locus, promoter)	This study
ML2055	$\Delta socB$; $P_{xyl-socB-YFP}::kan^R$ (<i>xyl</i> locus); $dnaN(G179C)-mCherry::gent^R$ (native locus, promoter)	This study
ML2056	$\Delta socAB$; $P_{van-socB-M2}::kan^R$; pMR20: $P_{xyl-socA}::tet^R$	This study
ML2057	$\Delta socB$; $P_{van-M2-socB}::kan^R$	This study
ML2058	$\Delta socB$; $clpX(Y76C)$; $P_{van-socB-M2}::kan^R$	This study
ML2059	$\Delta socB$; $clpX(Q232R)$; $P_{van-socB-M2}::kan^R$	This study
ML2060	$\Delta socAB$; $clpX(Y76C)$; $P_{van-socB-M2}::kan^R$; pMR20: P_{xyl-	This study

	<i>socA::tet^R</i>	
ML2061	$\Delta socAB$; <i>clpX(Q232R)</i> ; $P_{van-socB-M2}::kan^R$; pMR20: $P_{xyl-socA}::tet^R$	This study
ML2115	$\Delta socB$; $P_{xyl-socB(Q52A)}-YFP::kan^R$ (<i>xyl</i> locus)	This study
ML2116	pMR20: $P_{xyl-socB-GST-his6}::tet^R$	This study

EXTENDED EXPERIMENTAL PROCEDURES

Bacterial Strains and Media

Caulobacter strains were grown in PYE broth at 30°C unless otherwise indicated. To induce expression from the P_{xyI} , P_{van} , or P_{lac} promoters, media was supplemented with xylose (0.3%), vanillate (500 μ M), or IPTG (1 mM), respectively. For the P_{van} -*dnaN*-YFP and P_{van} -*dnaN*(G179C)-YFP strains, a lower concentration of vanillate (20 μ M) was used for induction. All chromosomal deletions were generated using a two-step recombination method and *sacB* as a counterselection marker (Skerker et al., 2005). The first and last five codons were left intact to prevent polar effects on downstream genes. Chromosomal integrations were performed using the pVGFPN/pXGFPN vectors that integrate at the P_{van} or P_{xyI} locus (Thanbichler et al., 2007). The pMR20 and pJS14 vectors were used for low- and medium-copy plasmid expression, respectively. Synchronizations of swarmer/G1 cells were performed using Percoll (GE Healthcare) density gradient centrifugation at 10,000g for 20 min.

Suppressor Screening and Mapping

To screen for suppressors of *clpP*, a *clpP* depletion strain (UJ199; Δ *clpP*; P_{xyI} -*clpP*) was transposon mutagenized using the EZ-Tn5 kit (Epicentre) and plated onto PYE medium containing glucose (to repress *clpP* expression) and kanamycin (25 μ g/ml, to select for transposon integration). Colonies that grew after 2-4 days were then isolated for genomic DNA extraction. To identify transposon insertion sites, genomic DNA from putative suppressor strains was digested, self-ligated, and transformed into *pir*-116 *E. coli*. Plasmids were prepped from the resulting transformants and sequenced using the Ez-Tn5 FP-1 forward primer.

To screen for suppressors of *socB*-M2 expression, a copy of *socB*-M2 was integrated at both the P_{van} and P_{xyI} loci to reduce the frequency of suppressor mutations that simply inactivate *socB*-M2. This strain was plated on PYE containing vanillate and xylose to induce *socB*-M2 expression. Colonies that grew after 2-3 days were screened for mutations within *socB* or *clpX* by directed sequencing, and for high levels of SocB-M2

expression by Western blotting. Strains without mutations in *socB* and *clpX* that expressed SocB-M2 were sent for whole-genome Illumina sequencing (BioMicroCenter, MIT). Illumina reads were mapped to the *Caulobacter crescentus* NA1000 reference genome using the bwa package and then sorted, indexed, and mutations called using the samtools package. Mutations were verified by directed sequencing.

Bacterial Two-Hybrid Assay

Protein interactions were assayed using the bacterial adenylate cyclase two-hybrid system (Karimova et al., 1998). Briefly, genes of interest were fused to the 3' or 5' end of the T18 or T25 fragments in the pUT18C pUT18C, pKT25, or pKNT25 vectors. The resulting T18- and T25-fusion plasmids were then co-transformed into BTH101 *E. coli*. Co-transformants were grown in M63 minimal media supplemented with maltose (0.2%), IPTG (1 mM, to induce the fusion proteins), and appropriate antibiotics. Saturated overnight cultures were then spotted onto MacConkey agar (40 g/L) plates supplemented with maltose (1%), IPTG (1 mM), and appropriate antibiotics. Plates were incubated at 30°C and pictures taken one or two days post-incubation.

Flow Cytometry

Caulobacter samples were fixed in 70% ethanol, pelleted at 4000 RPM, and then re-suspended in 50 mM sodium citrate containing 2 µg/ml RNase. Samples were then incubated for 4 hours at 50°C to digest RNA. Samples were diluted to an OD₆₀₀ of 0.001, stained with 2.5 µM SYTOX Green (Invitrogen), and then analyzed by flow cytometry on a BD Accuri C6 flow cytometer (BD Biosciences).

Protein Purification

All proteins were cloned into pET-based vectors for expression in BL21 *E. coli*. For purification of His6-SocB, cells were grown to OD 0.4 and then induced with 0.1 mM IPTG at 18°C overnight. Cell pellets were re-suspended in 20 ml prep buffer-20 (20 mM Tris-HCl pH 7.4, 500 mM NaCl, 20 mM imidazole, 10% glycerol) per liter of starting culture and lysed by sonication. Lysates were cleared by centrifugation at 17,000g for 1 hr, and then the cleared lysates were bound to Ni-NTA agarose for 1 hr in batch format

at 4°C. The Ni-NTA agarose was then applied to a 20 ml Econo-Pac chromatography column (Biorad), washed with five column volumes of prep buffer-20, and then eluted in 10 ml of prep buffer-250. His6-SocB was concentrated on an Amicon 10K Centrifugal Filter Unit (Millipore), buffer exchanged into PD-KCl-200 buffer (20 mM HEPES pH 7.6, 5 mM MgCl₂, 200 mM KCl, 0.032% NP-40, 10% glycerol) on PD-10 columns (GE Healthcare), and stored at -80°C. Due to low solubility at temperatures greater than 10°C, His6-SocB was always kept on ice after thawing. For purification of His6-SocA, expression was induced in BL21 *E. coli* that also contained the chaperone vectors pBB528 and pBB541 (de Marco, 2007), which we found greatly increased the yield of soluble His6-SocA protein. Otherwise, induction and purification conditions are identical as above, except that His6-SocA required further purification on a size exclusion column (S200, GE Healthcare) in order to remove high molecular weight contaminants. Fractions containing His6-SocA, as verified by Coomassie staining, were pooled and stored at -80°C. ClpX, ΔN-ClpX, and ClpP were generous gifts of Peter Chien (University of Massachusetts Amherst).

For proteins used in affinity chromatography experiments, purification conditions are identical as His6-SocB except for the differences noted below. For GST-His6 and DnaN-His6 (wild-type and mutant proteins), cells were grown to OD 0.4 and then induced with 0.3 mM IPTG at 30°C for 4 hr prior to collecting pellets. Purified and concentrated GST-His6 or DnaN-His6 was buffer exchanged into low salt buffer (20 mM Tris-HCl pH 7.4, 200 mM NaCl, 10% glycerol) and stored at -80°C. For GST-SocB-His6 (wild-type and mutant proteins), cells were grown to OD 0.4 and then induced with 0.1 mM IPTG at 18°C overnight. Purified and concentrated GST-SocB-His6 was buffer exchanged into low salt buffer and stored at -80°C.

Affinity Chromatography

For binding assays, 100 μl of glutathione sepharose 4B beads (GE Healthcare) was pre-washed in binding buffer (50 mM HEPES-KOH pH 7.5, 100 mM KCl, 0.1 mM EDTA, 2.5 mM MgCl₂, 3% glycerol, 0.1% Triton X-100). Washed beads were then incubated with 1 mg of GST-tagged protein for 1.5 hr at 4°C with rotation. Beads were washed twice with 1 ml of binding buffer, and then 0.25 mg of bait protein (DnaN-His6 wild-type

or mutant protein) was added and allowed to bind for an additional 1.5 hr. Beads were then transferred to a 10 ml Poly-Prep chromatography column (BioRad) and then washed with six column volumes of binding buffer. Columns were capped and then 100 μ l of elution buffer (50 mM Tris-HCl pH 8.0, 40 mM reduced glutathione) was added. After 30 min incubation, eluates were collected. An equal amount of protein was loaded on each lane of an SDS-PAGE gel and proteins were visualized by Coomassie blue staining.

Microscopy and Image Analysis

Differential interference contrast (DIC) and fluorescence images were taken using a Zeiss Axiovert 200 microscope with a 100x/1.45 oil immersion objective. Phase contrast images and time-lapse movies were taken on a Zeiss Observer Z1 microscope using a 100x/1.4 oil immersion objective and an LED-based Colibri illumination system. Cells were placed on a PYE + 1.5% low-melting agarose pad supplemented with xylose or vanillate as indicated, and imaged in a glass-bottomed petri dish wrapped with Parafilm to prevent desiccation. Pictures were taken every 5 minutes, and temperature was maintained at 30°C using the Zeiss Temp Module S1 and Heating Insert P S1. Automatic focusing was performed using the Zeiss Definite Focus module. To perform cell segmentation and tracking, images were processed using MicrobeTracker (Sliusarenko et al., 2011). Position of the DnaN-YFP focus along the cell axis was determined using custom-written MATLAB software. Briefly, fluorescence along the cell axis was extracted and fit to a smoothing spline. Presence of a focus was determined by looking for local minima in the second derivative of the smoothing spline that crossed below a pre-determined threshold. Cells were scored if (1) they had no focus in the first frame, and (2) a focus was observed to form at some point later in the movie. To calculate n_{focus} , the location of the focus was plotted as a function of time, and a smoothing spline was fit to its trajectory. The average of the absolute value of the first derivative of this smoothing spline was taken as n_{focus} . To calculate t_{focus} , the time from focus appearance (defined as the first frame with a focus) to disappearance (defined as the first frame with a focus for which the following two frames have no focus) was calculated.

To calculate percentage of cells with SocB-YFP foci, the fluorescence along the cell axis was extracted and fit to a smoothing spline. Foci were defined as local minimum that crossed below a pre-determined threshold in the second derivative. To calculate co-localization between SocB-YFP and DnaN-mCherry, the same foci scoring function was used as above to determine the position of any SocB-YFP or DnaN-mCherry foci in the cell. If the position of the highest scoring DnaN-mCherry peak (as determined by lowest local minimum in the second derivative) and a SocB-YFP peak overlapped, the cell was classified as exhibiting co-localization.

SUPPLEMENTAL REFERENCES

de Marco, A. (2007). Protocol for preparing proteins with improved solubility by co-expressing with molecular chaperones in *Escherichia coli*. *Nat. Protoc.* 2, 2632-2639.

Jenal, U., and Fuchs, T. (1998). An essential protease involved in bacterial cell-cycle control. *EMBO J.* 17, 5658-5669.

Sliusarenko, O., Heinritz, J., Emonet, T., and Jacobs-Wagner, C. (2011). High-throughput, subpixel precision analysis of bacterial morphogenesis and intracellular spatio-temporal dynamics. *Mol. Microbiol.* 80, 612-627.